BULLETIN OF THE POLISH ACADEMY OF SCIENCES
TECHNICAL SCIENCES, Vol. 66, No. 6, 2018
DOI: 10.24425/bpas.2018.125946

Fractional order based velocity control system for a nanorobot in non-Newtonian fluids

C.I. MURESAN[1], I.R. BIRS[1]*, S. FOLEA[1], and C. IONESCU[1,2]

[1]Technical University of Cluj-Napoca, Romania
[2]Ghent University, Belgium

Abstract. Customized patient drug delivery overcomes classic medicine setbacks such as side effects, improper drug absorption or slow action. Nanorobots can be successfully used for targeted patient-specific drug administration, but they must be reliable in the entire circulatory system environment. This paper analyzes the possibility of fractional order control applied to the nanomedicine field. The parameters of a fractional order proportional integral controller are determined with the purpose of controlling the velocity of the nanorobot in non-Newtonian fluids envisioning the blood flow in the circulatory system.

Key words: non-Newtonian fluids, drag forces, velocity control, fractional calculus.

1. Introduction

Several possibilities of defining real or complex number powers of the differentiation and integration operators have been intensely studied in the last years. The popularity of fractional calculus has increased in the control engineering field in the areas of process modeling and controller tuning such as the fractional order proportional integrative derivative (FOPID) controller [1–3]. The results obtained by using fractional operators consisted of more accurate modeling of physical phenomena and obtaining controllers that performed better when compared to the classic PID controller [4]. In the case of the fractional order PID, there are more parameters to be tuned than the integer order. The tuning of the controller is usually done by solving a system of equations in the frequency domain involving the phase margin, gain crossover frequency and robustness [5–7].

Newton's law of viscosity is the ability of a fluid to resist gradual deformation caused by shear of tensile stresses. A non-Newtonian fluid is dependent on shear rate and shear rate history. Non-Newtonian fluids can be modeled using the Navier-Stokes equation over linearized interval, which may become obsolete at limit flows [8]. One classic example of such a fluid is the blood. One dimensional blood flow can be successfully modeled using fractional order operators. The interplay between viscous dissipations and elastic energy storage is modelled through a single fractional order parameter α [9]. A physically accurate model for the blood flow brings great improvements in understanding and improving the nanomedicine field. Nanotechnology is currently used for targeted drug delivery that overcomes the problems encountered in classic medicine. There are cases in which the solubility properties of the drug are low and the body struggles to absorb enough. Also, the drug may have the proper solubility, but the body removes it before it has enough time to provide benefits. There is also the issue of side effects caused by excessive substance or poor delivery of it at the site of the diseases. For example, cancer targeted drugs must act solely on the affected cells and ignore the healthy tissue. Nanomedicine can play an important role in eliminating side effects, provide faster action and improving the quality of the treatment [10–13]. The real-life applicability with its drawbacks and difficulties such as body rejection and determining the particular treatment scheme for individual patients are described in [12].

The paper presents some preliminary results regarding the design of a velocity control system for a nanorobot in non-Newtonian fluids. Since previous research has shown that the characteristics of non-Newtonian fluids are better represented using fractional order models [8], the velocity control system is also based on a fractional order controller. When compared to a classical, integer-order controller, fractional order approaches in control strategies prove superior in terms of stability, robustness and honoring design specifications [14, 15].

The paper is structured as follows. After the Introduction, the second section describes the dedicated experimental platform that will be further used to validate the results presented in this paper. The third section describes the design of a fractional order controller, whereas the actual tuning of this controller for the nanorobot velocity is detailed in section four. Finally, some concluding remarks are presented in the last section, as well as some future research ideas.

2. Towards a dedicated experimental platform

2.1. Design of the test stand. The circulatory system simulator is realized based on the myRIO^{TM} equipment, which is LabVIEW^{TM} programmable.

*e-mail: Isabela.Birs@aut.utcluj.ro

Manuscript submitted 2017-11-19, revised 2018-02-14, initially accepted for publication 2018-02-21, published in December 2018.

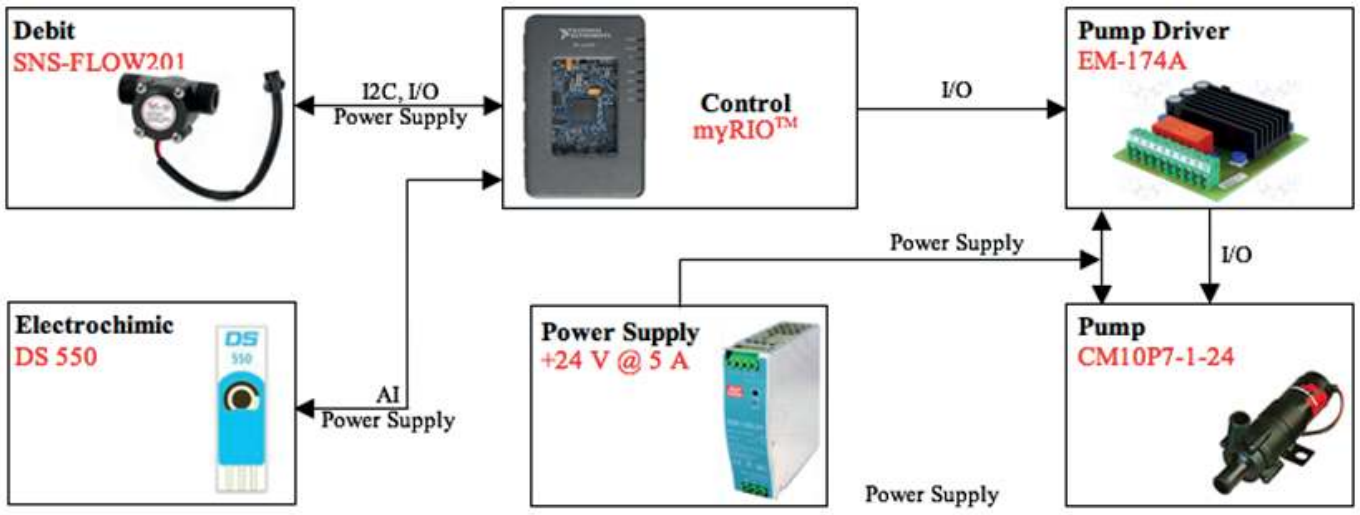

Fig. 1. Experimental setup – hardware block diagram

The system consists of analog and digital lines, serial interfaces of UART type, I^{2}C or SPI, Wi-Fi and USB communication (master and slave) as can be seen in the diagram from Fig. 1.

Among the advantages there are: flexibility, ease of programming programmable (because of the graphic programming language) and real-time performance given by the operating system and the integrated FPGA (Field Programmable Gate Arrays).

The design of the test stand is detailed in Fig. 2. The variable flow pump CM10P7–1–24 ensures a variable flow and a similar profile as the one in the circulatory system. The pump needs +24 V and can generate a flow of up to 15 liters per minute. The driver for the pump, EM-174A, allows a variable or continuous command of the flow and needs between +10 V and +35 V to operate.

Closing the control loop is possible because of the flowmeter SNS-FLOW201 with a flow between 1 and 30 liters in a minute. The supply voltage is 5–18 V while the output is a TTL frequency signal.

The concentration is measured with 3 electrodes (CE, RE, WE) of type DS 550 and dedicated electronics that ensures a certain impedance, reference signal generation and signal processing. The integration of the module in the submersible is limited because of the circuit dimensions and the necessity of a supply voltage between 10 V and 15 V that requires another 2 commutation circuits. In the implemented configuration, the myRIO^{TM} controller gives the supply voltage of ±15.0 V.

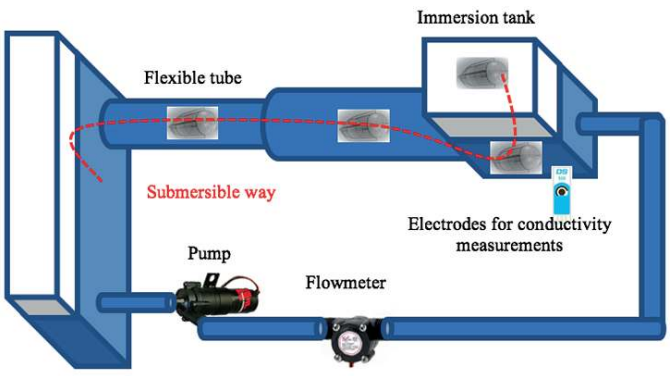

Fig. 2. Test stand – design

2.2. Design of the submersible. The submersible device has one motor for propulsion with a propeller bigger than the fuselage that can rotate in both directions. The propeller can generate a current in the fluid helping the submersible move forward and it can also produce a contra current such that the submersible is not moved by the flow of the liquid.

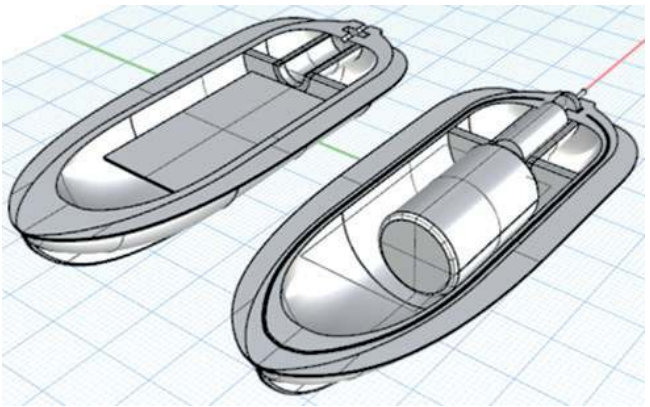

Fig. 3. Submersible – longitudinal section

A longitudinal section through the submersible is presented in Fig. 3. On the left side is the board containing all the electronics, while on the right side is the battery and the motor which are separated in isolated compartments.

The command of the submersible is realized based on the ESP WROOM-02 Arduino programmable module. This module offers analogic and digital lines, UART, I^{2}C or SPI and the

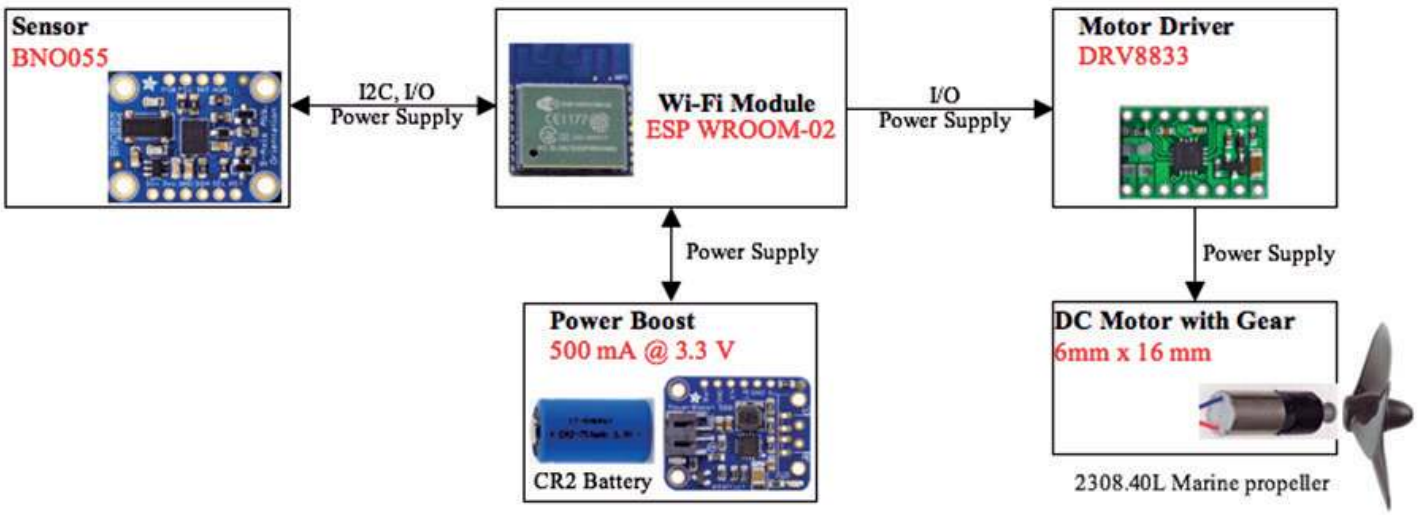

Fig. 4. Experimental setup – submersible hardware block diagram

wireless communication (Fig. 4). The advantages of integrating this module are: reduced dimension, low power consumption, ease of programming, support for special functions and the communication stack.

The position is determined using the BNO055 circuit which includes three types of sensors: accelerometer, gyroscope and magnetometer.

By fusing data from the 9-DOF device, a precise positioning is obtained. The position algorithm is based on double integrating the linear acceleration provided by the BNO sensor fusion. The proposed algorithm for double integration in the case of the acceleration and overcoming the accumulating error is presented in [16]. The study presents the integration algorithm as well as experimental validation of the method in order to confirm that the obtained accuracy can be for the same electronic equipment and the same submersible as the one presented in this paper.

The propulsion is realized by a continuous current motor with a 25:1 gearbox. The angular velocity is 1650 rpm, the diameter is 6mm, the length is 16mm and the supply voltage is 3 V. The driver for the DC motor is realized with the DRV8833 used for setting the rotation direction and sudden breaking.

The presented setup presented in Fig. 3. is fed from a CR2 3 V lithium battery and has a capacity of up to 850 mAh. A booster circuit has been included, TPS61090, to ensure 3.3 V operating voltage. Usually, the lithium batteries have a plain characteristic, giving a nominal voltage between 2.7 and 3.0 V for a long period of type. The ESP WROOM-02 has a minimum limit of 3.0 V and, without this circuit, the proper operating voltage can't be assured.

Since the communication with the entire setup is done over WiFi, there is a network delay present. Weather this delay is constant or not is irrelevant since the shared information is related to the current position of the submersible. The control algorithm is implemented on the microcontroller and the control signal is computed inside the submersible, without needing any additional information sent over the network.

A significant improvement to the presented setup is including the circuit that measures the fluid conductivity at the submersible level. The current setup is modular, but the final version will have dedicated electronics, reducing considerably the size of the setup.

3. Design of a fractional order based velocity controller

For zero steady state errors in the velocity profile of the nanorobot, an integrative effect of the controller is required. This implies a fractional order PI controller design for velocity control. The transfer function of this controller is given as:

$$H_{FO-PI}(s) = k_p\left(1 + \frac{k_i}{s^{\mu}}\right) \tag{1}$$

with $\mu \in (1, 0)$ the fractional order, s – the Laplace variable, and k_p and k_i – the proportional and integral gains. Once the structure of the controller has been established in the form given in (1), the design of the controller implies the tuning of the three controller parameters k_p, k_i and μ. The tuning is based on a set of closed loop performance constraints that the overall nanorobot system must meet. In this particular case, the robustness is one of the key issues and this constraint represents the most important requirement for the nanorobot control system. Apart from the robustness constraint, the nanorobot velocity control system should exhibit a fast settling time and a low overshoot. Thus, for the tuning of the fractional order PI controller the following design specifications are considered:

3.1. Robustness. This design constraint implies that the overall nanorobot control system ensures similar closed loop performance despite possible modeling errors, disturbances, uncertainties, parameter variations, etc. In this paper, the open loop

gain variations are considered only. To make the overall closed loop system robust to these variations, the corresponding open loop system should have a flat phase around the gain crossover frequency, ω_{gc}. In this way, the phase margin, φ_m, remains constant and the closed loop system will behave in a similar manner regardless of possible variations in the system gain. This design constraint can be specified in the frequency domain as:

$$\left.\frac{d\left(\angle H_d(j\omega)\right)}{d\omega}\right|_{\omega=\omega_{gc}} = 0 \tag{2}$$

where $H_d(s) = H_P(s) \cdot H_{FO-PI}(s)$ is the open loop system transfer function with $H_P(s)$ is a transfer function that describes the relation between the nanorobot velocity and the power supplied to the propeller system.

3.2. Settling time. For the velocity control system to be effective, the settling time of the overall closed loop system must be fast enough so that the nanorobot will be able to track the desired speed as fast as possible, without traveling too much down the blood vessels. In this paper, the aim is to reduce by five times the average settling time of the nanorobot velocity system. The settling time requirement is treated indirectly by specifying a certain gain crossover frequency as the design constraint. In the frequency domain, this requirement implies:

$$\left|H_d(j\omega_{gc})\right| = 1 \tag{3}$$

where $|.|$ stands for the modulus of a transfer function.

3.3. Overshoot. The velocity control system of the nanorobot should exhibit a reduced overshoot. In frequency domain, this requirement is tackled using the phase margin performance specification. A large phase margin will be imposed as a design constraint and leads to a reduced overshoot. This performance criteria is specified as:

$$\angle H_d(j\omega_{gc}) = -\pi + \varphi_m \tag{4}$$

where $\angle \cdot$ represents the phase of a transfer function.

In what follows, without loss of generality, we assume that the velocity of the nanorobot can be written in its Laplace form as:

$$H_P(j\omega_{gc}) = \frac{1}{K + jL} \tag{5}$$

where K and L denote the real and imaginary parts and are both functions of the frequency ω.

The frequency domain representation of the transfer function of the fractional order PI controller in (1) can be expressed as follows, taking $s \to j\omega_{gc}$:

$$H_{FO-PI}(j\omega_{gc}) = k_p\left[1 + k_i\omega_{gc}^{-\mu}\left(\cos\frac{\pi\mu}{2} - j\sin\frac{\pi\mu}{2}\right)\right]. \tag{6}$$

According to (5) and (6), the phase of the open loop transfer function can be computed simply as:

$$\angle H_d(j\omega_{gc}) = \tan^{-1}\left(-\frac{k_i\omega_{gc}^{-\mu}\sin\frac{\pi\mu}{2}}{1 + k_i\omega_{gc}^{-\mu}\cos\frac{\pi\mu}{2}}\right) - \tan^{-1}\left(\frac{L}{K}\right). \tag{7}$$

Replacing now (7) into (4) leads to:

$$\tan^{-1}\left(-\frac{k_i\omega_{gc}^{-\mu}\sin\frac{\pi\mu}{2}}{1 + k_i\omega_{gc}^{-\mu}\cos\frac{\pi\mu}{2}}\right) - \tan^{-1}\left(\frac{L}{K}\right) = -\pi + \varphi_m. \tag{8}$$

Separating the terms and applying the tangent function to (8) leads to:

$$\frac{k_i\sin\left(\frac{\pi\cdot\mu}{2}\right)}{\omega_{gc}^{\mu} + k_i\cos\left(\frac{\pi\cdot\mu}{2}\right)} = tg\left(\pi - \varphi_m - a\tan\left(\frac{L}{K}\right)\right). \tag{9}$$

Using the result in (7) to apply the derivative with respect to the frequency ω as indicated in (2), leads to:

$$\frac{\mu k_i\omega_{gc}^{-\mu-1}\sin\frac{\pi\mu}{2}}{1 + 2k_i\omega_{gc}^{-\mu}\cos\frac{\pi\mu}{2} + k_i^2\omega_{gc}^{-2\mu}} - \frac{\dot{L}K - L\dot{K}}{L^2 + K^2} = 0. \tag{10}$$

Equations (9) and (10) can now be used to uniquely determine the parameters k_i and μ of the fractional order PI controller. This can be simply achieved using graphical methods in which the k_i parameter computed based on (9) is plotted as a function of the fractional order μ. The procedure is repeated for k_i computed based on (10). The result of this approach consists in two plots of k_i as functions of μ. Thus, the final solution of (9) and (10) can be found at the intersection of the two plots [8].

Once the k_i and μ parameters have been computed, the settling time condition specified as the modulus equation in (3) is used to determine the last parameter k_p:

$$\left|\frac{1}{k + jL}\right|_{\omega_{gc}}\left|k_p\left[1 + k_i\omega_{gc}^{-\mu}\left(\cos\frac{\pi\mu}{2} - j\sin\frac{\pi\mu}{2}\right)\right]\right| = 1. \tag{11}$$

The proportional gain k_p can be computed using (11):

$$k_p = \frac{\sqrt{L^2 + K^2}}{\sqrt{1 + 2k_i\omega_{gc}^{-\mu}\cos\frac{\pi\mu}{2} + k_i^2\omega_{gc}^{-2\mu}}}. \tag{12}$$

4. Main results

Information regarding nonlinear parametric models can be obtained by analyzing the shear rate as being dependent on the viscosity of the blood [8, 17].

Linear transfer functions with variable parameters can be obtained through linearization. The pole-zero mappings of the obtained transfer functions vary significantly if a full coverage of the flow dynamics is desired. The dominant lead-lag is changed through drag forces in the hemodynamic time-space. Taking the case of a single particle and analyzing its moving from the hemodynamic point of view, the obtained dominant poles is real, while the zeroes are complex conjugated.

The gradient in the values of the pole-zero mappings is a fifth-fold order of magnitude. Figure 5 presents the 5th order frequency response of the gradient taking into consideration the particle's acceleration rate caused when exposed to pressure changes. Taking the real conditions of the circulatory system gives an operating environment in which the temperature is 37°C in a blood viscosity of 3–4 mPa second [18]. In addition, the heart beats 70 to 100 times in a second providing a frequency range of interest below 100 rad/s. Analyzing the data presented in Fig. 5 it can be seen that the time constant response varies significantly implying that the particle has a very high acceleration or very low movement. From the control effort point of view, the controller must ensure constant acceleration in the divergent environment. Practical implementation must take into consideration tuning the controller using robustness constraints such that the performance of the obtained controller overcomes the bandwidth limitation.

In this paper, a fractional order PI (FO-PI) controller is designed to meet the requirements regarding the isodamping property (robustness to open loop gain variations). Additionally, to reduce the settling time and ensure a low overshoot, the open loop gain crossover frequency is selected as ω_{cg} =0.85 rad/s, while the phase margin is $\varphi = 73°$.

The linear model for which this controller is designed is given as:

$$H_P(s) = \\ = \frac{2493(s+626.2)(s^2+2.188s+111.5)}{(s+53.32)(s+0.09916)(s^2+586.6s+197500)}. \quad (13)$$

The Bode diagram and the step response of (13) are given in Fig. 5 and 6, respectively. The transfer function in (13) in its complex form is:

$$H_P(j\omega_{gc}) = \frac{1}{0.006+0.0517j} \quad (14)$$

with the modulus equal to 25.66 dB and the phase −83.36°. These results can be easily verified on the Bode diagram. The step response shows zero overshoot and a settling time of 39.5 ms.

Figure 7 shows the plots of the k_i parameter as a function of the fractional order μ as resulting from the isodamping and phase margin design constraints in (9) and (10). The intersection in Fig. 7 gives the following result: $\mu = 0.5217$ and $k_i = 0.9035$. With this values replaced into (12), the proportional gain is determined to be: $k_p = 0.0282$.

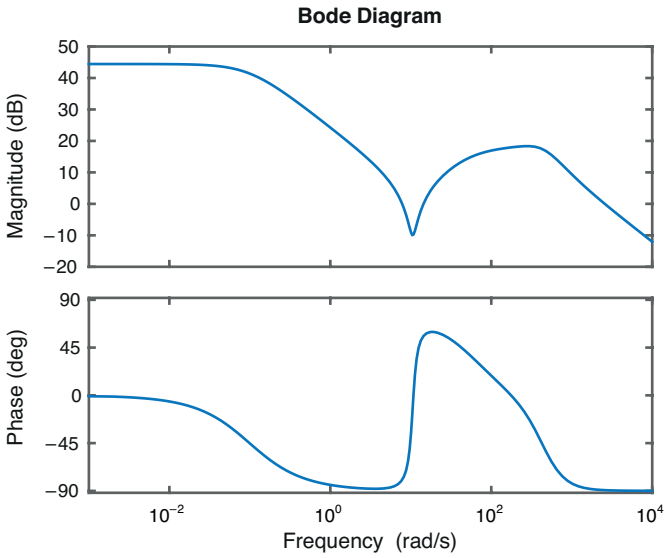

Fig. 5. Bode diagram of the linear model used in the design of the velocity control system

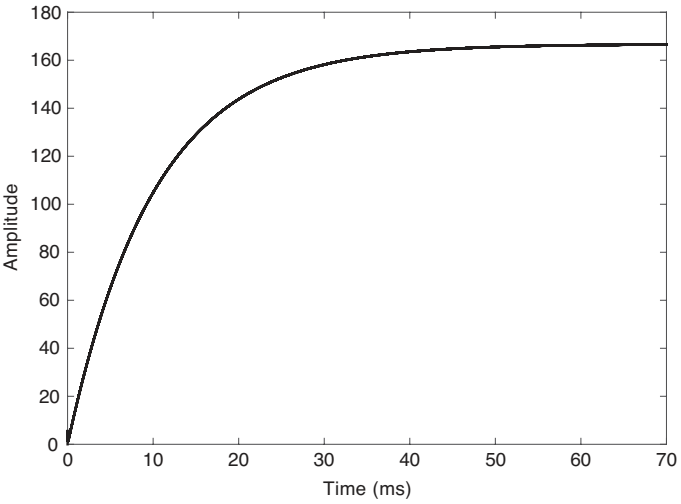

Fig.6. Step response of the linear model used in the design of the velocity control system

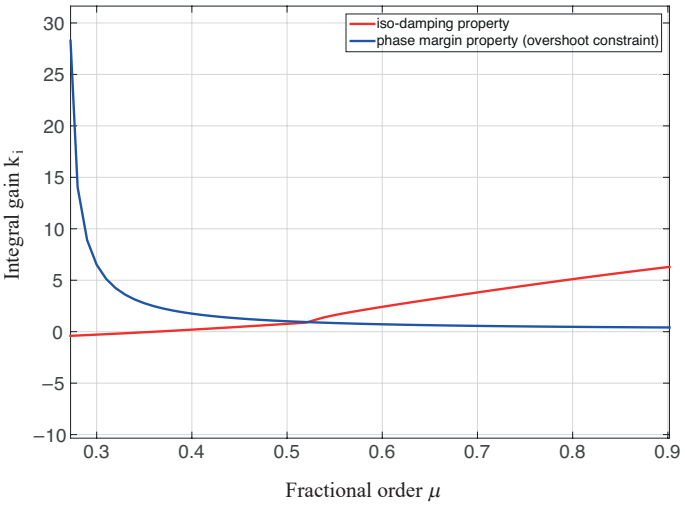

Fig. 7. Plots of k_i as functions of the fractional order μ

The transfer function of the FO-PI controller is finally:

$$H_{FO-PI}(s) = 0.0282\left(1 + \frac{0.9305}{s^{0.5217}}\right). \tag{15}$$

The Bode diagram of the open loop system, showing that all design specifications are met, is given in Fig. 8, as well as the frequency response of the system considering ±30% gain variations. Figure 10 indicates the closed loop simulation results considering both the nominal, as well as ±30% gain variations. The simulation results show a reduced overshoot, regardless of the open loop gain variations. This is due to a constant phase margin as indicated in Fig. 9. It is obvious that the designed

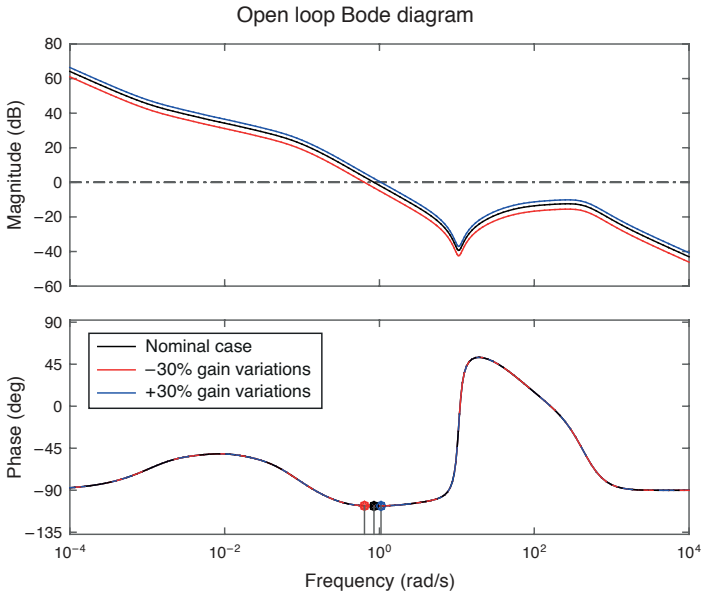

Fig. 8. Bode diagram of the open loop system

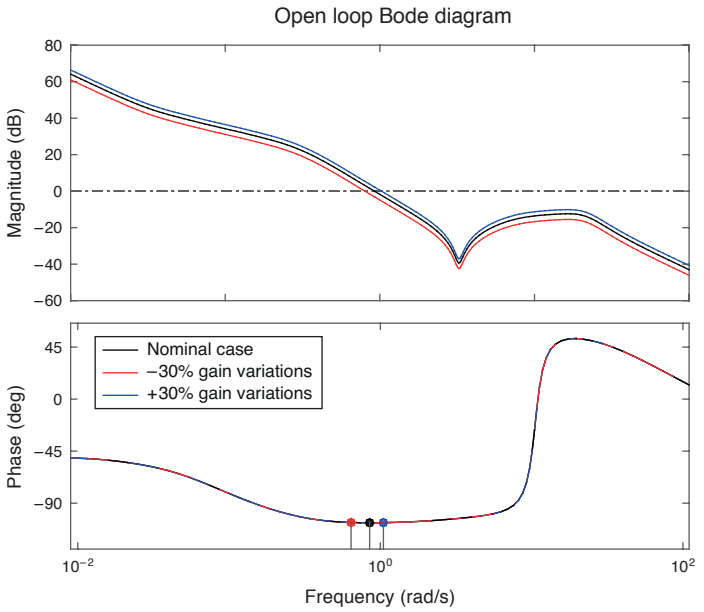

Fig. 9. Bode diagram of the open loop system – highlight on the robustness characteristic

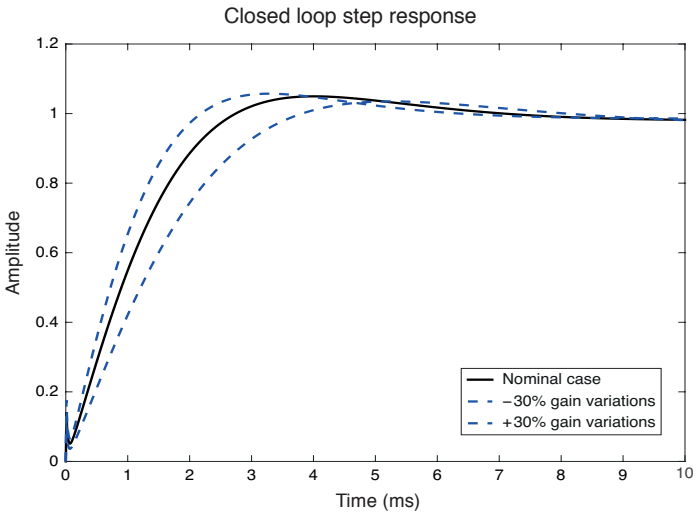

Fig. 10. Closed loop step response

fractional order controller has significantly reduced the settling time, with the nominal velocity control system reaching its final steady state value within 5.86 ms and 5.14 ms and 6.75 ms in the case of ±30% gain variations. As specified in the design constraint, the settling time is reduced by more than five times with respect to the open loop system.

5. Conclusions

The purpose of the presented work is to design a fractional order controller that ensures a constant velocity of a nanorobot moving through the circulatory system. The submersible must overcome the hostile environment from the blood flow, which exhibits the behavior of a non-Netwonian fluid.

A fractional order PI controller is obtained based on imposed frequency domain specifications such as gain crossover frequency, phase margin and the isodamping property. The obtained controller significantly reduces the settling time and overshoot and ensures robustness to gain variations.

The results obtained prove that fractional order calculus can be successfully applied to the nanomedicie field bringing improvements in targeted patient-specific drug delivery.

Acknowledgements. This work was supported by a grant of the Romanian National Authority for Scientific Research and Innovation, CNCS/CCCDI-UEFISCDI, project number PN-II-P2–2.1-PED-2016–0101, with PNCDI III.

References

[1] C. Ionescu, P. Segers, and R. De Keyser, "Mechanical properties of the respiratory system derived from morphologic insight", *IEEE Trans. Biomed. Eng.* 56, 949–959 (2009).

[2] C. Ionescu and R. De Keyser, "Relations between fractional order model parameters and lung pathology in chronic obstructive pulmonary disease", *IEEE Trans. Biomed. Eng.* 56, 978–987 (2009).

[3] F. Mainardi, "Fractional calculus and waves in linear viscoelasticity: An introduction to mathematical models", Imperial College Press, London, 2010.
[4] C.A. Monje, Y. Chen, B.M. Vinagre, D. Xue, and V. Feliu, "Fractional- order systems and controls: Fundamentals and applications", Springer, London, 2010.
[5] C.I. Pop, C.M. Ionescu, R. De Keyser, E.H. Dulf, and E.-H, "Robustness evaluation of Fractional Order Control for Varying Time Delay Processes", *Signal, Image and Video Processing*. 6, 453–461 (2012).
[6] A. Oustaloup, "La commande CRONE: commande robust d'ordre non entiere", Hermes, Paris, France, 1991.
[7] C.A. Monje, B. Vinagre, Y. Chen, and V. Feliu, "On fractional PI^{λ} controllers: some tuning rules for robustness to plant uncertainties", *Nonlinear Dyn*. 38, 369–381 (2004).
[8] C.M. Ionescu, "A memory-based model for blood viscozity", *Commun. Nonlinear Sci. Numer. Simul*. 45, 29–34 (2017).
[9] P. Perdikaris and G.E. Karniadakis, "Fractional-order viscoelasticity in one-dimensional blood flow models". *Annals of Biomedical Engineering* 42 (5), 1012–1023 (2012).
[10] Y. Liu, H. Miyoshi, and M. Nakamura, "Nanomedicine for drug delivery and imaging: a promising avenue for cancer therapy and diagnosis using targeted functional nanoparticles". *Int. J. Cancer* 120, 2527–2537 (2007).
[11] V. Jain, S. Jain, and S.C. Mahajan, "Nanomedicines based drug delivery systems for anti-cancer targeting and treatment". *Curr Drug Deliv*. 12(2), 177–91 (2015).
[12] P. Debbage, "Targeted drugs and nanomedicine: present and future", *CurrPharm Des* 2009; 15:153–72.
[13] V.K. Khanna, "Targeted delivery of nanomedicines". *ISRN Pharmacology*, 2012, 2012, 1–9.
[14] J.A.T. Machado, A. Galhano, and J.J. Trujillo, "On development of fractional calculus during the last fifty years." *Scientometrics* 98, 577–582 (2013).
[15] W. Jifeng and L. Yuankai, "Frequency domain anal- ysis and applications for fractional-order control systems", *Journal of Physics: Conference Series* 13 (1), 2005.
[16] I. Birs, C. Muresan, S. Folea, and O. Prodan, "An Experimental Nanomedical Platform for Controller Validation on Targeted Drug Delivery", Australian and New Zealand Control Conference (ANZCC), 17–20 December 2017, Gold Coast, Australia.
[17] S.N. Doost, L. Zhong, B. Su, and Y.S. Morsi, "The numerical analysis of non-Newtonian blood flow in human patient-specific left ventricle", *Comput. Methods Programs Biomed*. 127, 232–247 (2016).
[18] M. Sanak, B. Jakiela, and W. Wegrzyn, "Assessment of hemocompatibility of materials with arterial blood ow by platelet functional", *Bull. Pol. Ac:. Tech*. 58(2), 317–322 (2010).